Eur. J. Mineral., 38, 237–247, 2026
https://doi.org/10.5194/ejm-38-237-2026

European Journal of Mineralogy
Open Access

Erzwiesite, $Ag_8Pb_{12}Bi_{16}S_{40}$, the natural orthorhombic $N = 8$ member of the lillianite homologous series

Dan Topa[1], Emil Makovicky[2], Hubert Putz[3], Werner Hermann Paar[4], and Georg Zagler[5]

[1]Mineralogisch-Petrographische Abteilung, Naturhistorisches Museum, Burgring 7, 1010 Wien, Austria
[2]Department of Geoscience and Resource Management, University of Copenhagen, Østervoldgade 10, 1350, Copenhagen K, Denmark
[3]Salletmayr & Friedl Ziviltechniker GmbH, Karl-Lötsch Straße 10, 4840 Vöcklabruck, Austria
[4]Pezoltgasse 46, 5020 Salzburg, Austria
[5]Brandirn 21, 5222 Munderfing, Austria

Correspondence: Dan Topa (dan.topa@nhm.at)

Received: 22 December 2025 – Revised: 7 April 2026 – Accepted: 8 April 2026 – Published: 29 April 2026

Abstract. Erzwiesite, ideally $Ag_8Pb_{12}Bi_{16}S_{40}$, $Z = 1$, is a new sulfosalt mineral discovered in the Erzwies mining area, Gastein Valley, Salzburg Province, Austria. The mineral occurs as small black, irregular needle-like crystals mixed with galena and heyrovskýite in a quartz matrix. In reflected light, erzwiesite is greyish white. Under crossed polars it is distinctly anisotropic, and the rotation tints change from pale brown to pale bluish grey to dark brown. Reflectance measurements in air yield the following R_{min}/R_{max} values based on the standard wavelengths (Commission on Ore Mineralogy, COM): 44.5/47.6 (470 nm), 41.9/45.0 (546 nm), 41.5/44.5 (589 nm), and 40.4/43.6 (650 nm). The Mohs' hardness is 3–3.5 (VHN_{50} ranges from 195 to 224, mean 210 kg mm^{-2}). Averaged electron-microprobe analyses ($n = 6$) gave (in wt %) Ag 11.10(27), Cu 0.04(3), Pb 29.50(77), Cd 0.17(1), Bi 42.90(63), Te 0.21(14), Se 0.08(5), and S 16.08(11), with a total of 100.10(63). The empirical formula is $Ag_{8.18}Cu_{0.05}Pb_{11.31}Cd_{0.12}Bi_{16.30}Sb_{0.01}S_{39.81}Te_{0.13}Se_{0.06}$ (based on 76 apfu). The calculated density is 7.075 g cm^{-3} using the empirical formula. Erzwiesite crystallises in space group *Cmcm* ($a = 4.085(5)$, $b = 13.462(15)$, $c = 33.92(4)$ Å, and $V = 1866(4)$ Å^3). The crystal structure was determined from single-crystal X-ray diffraction data ($R_1 = 5.24$ % for 308 data with $F_o > 4\sigma(F_o)$ and 51 variable parameters). The structural formula is $Ag_{8.64}Pb_{11.04}Bi_{16.32}S_{40}$. The seven strongest lines in the X-ray powder diagram are [d in Å (intensity) *hkl*] 3.588 (64) 028, 3.387 (98) 115, 3.349 (37) 041, 3.288 (85) 029, 2.919 (100)133, 2.846 (99)134, and 2.039(43) 157. Erzwiesite is the first natural (8 : 8) homologue of the lillianite homologous series and is named after its type locality.

1 Introduction

The lillianite homologous series (LHS), defined by Makovicky and Karup-Møller (1977a, b), contains structures composed of $(311)_{PbS}$ slabs of galena-like structure. Adjacent slabs are in a mirror-related orientation; in most cases these adjacent slabs are of the same thickness, but phases with different thicknesses of adjacent mirror-oriented slabs are known as well, resulting in their regular alternation (Ferraris et al., 2008; Makovicky, 2006).

The order of the homologue is determined by the number of cation coordination octahedra in a string running diagonally through an individual slab. The Pb–Ag–Bi sulfides start with $N = 4$, and known cases reach $N = 11$. The general formula of these homologues is $Ag_xPb_{N-1-2x}Bi_{2+x}S_{N+2}$ ($Z = 4$), where N is the "chemical" value of N that for ideal chemical analysis is equal to $(N_1 + N_2)/2$, and N_1 and N_2 are the structural values of N for the two sets of slabs related by (partial) reflection across composition planes and can be equal ($N_1 = N_2$) or different ($N_1 \neq N_2$). The subscript x in the formula is the coefficient of $Ag + Bi \leftrightarrow 2Pb$ substitution

(Makovicky and Karup-Møller, 1977a). Hence, the lillianite homologue can be written as ${}^{N1,N2}\mathrm{L}$ when N_1 and N_2 are known from structure study or as ${}^{N_{\mathrm{chem}}}\mathrm{L}$ when only chemical data are known. The molar fraction of the Ag–Bi end member (due to $2\mathrm{Pb}^{2+}$ for the $\mathrm{Ag}^{+} + \mathrm{Bi}^{3+}$ substitution mechanism) is defined as substitution percentage (Subst. %). The general formula can be recast into an equation giving the value of N_{chem}, based on empirical contents of Pb(Cd), Bi(Sb), and Ag(Cu) as a tool for mineralogical determination of lillianite homologues (Makovicky and Karup-Møller, 1977a, b; Ferraris et al., 2008). When, as is often the case, only chemical data are available, the studied grain can be characterised as ${}^{N_{\mathrm{chem}}}\mathrm{L}_{\mathrm{Subst}}$. The analytical formulae for N_{chem}, Subst. %, and x are given in Makovicky and Karup-Møller (1977a). The above-mentioned observations by Makovicky and Karup-Møller (1977b) led to a limited spectrum of lillianite homologues known in the Pb–Bi–Ag–S system, ${}^{4,4}\mathrm{L}$, ${}^{4,7}\mathrm{L}$, ${}^{7,7}\mathrm{L}$, ${}^{5,9}\mathrm{L}$, ${}^{4,8}\mathrm{L}$, and ${}^{11,11}\mathrm{L}$, which were either confirmed by structure determination or derived by strict geometrical considerations (Table 1.1 in Ferraris et al., 2008).

In the last decade, a synthetic ${}^{8}\mathrm{L}_{70}$ phase was described by Topa et al. (2010), and a review of the LHS was given by Makovicky and Topa (2014). Recently, a new mineral, tarutinoite – a natural ${}^{7.5}\mathrm{L}_{54}$ member of the series – was described by Kasatkin et al. (2025).

During the detailed investigation of the material from the Erzwies mining area, we found a phase with chemistry and crystal structure close to those of the synthetic orthorhombic $N = 8$ member of the lillianite homologous series. The new phase described below increases the number of minerals with chemistry and crystal structure related to the lillianite homologous series.

The name erzwiesite (Erw) is for the middle-age gold mining place, the Erzwies mining area, Gastein Valley, Salzburg Province, Austria.

The mineral and mineral name have been approved by the Commission on New Minerals Nomenclature and Classification (CNMNC) of the International Mineralogical Association (IMA 2012-082, Topa et al., 2013). The holotype specimen, consisting of a hand specimen and a polished sample, was deposited in the mineralogical collection of the Natural History Museum, Wien, Austria, under catalogue no. O 2407.

2 Occurrence and paragenesis

Erzwiesite occurs as a very rare constituent in several samples from an unnamed prospect at 2390 m above sea level in the Erzwies mining district, Gastein Valley, Salzburg Province, Austria (47°5′40″ N, 13°2′15″ E). Au- and Ag-bearing mineralisation in this area is linked to the so-called "Kupelwieser" vein, which represents one of the NNE-striking structures of the "Tauerngold vein" type in the Rauris–Gastein mining district. The abovementioned structure is hosted by either Variscan granitoids (the so-called "Zentralgneis") or metasediments of Jurassic age; the latter is characterised by numerous karst phenomena (Höfer, 2001, 2005). The "Kupelwieser" structure is accompanied by numerous NE–SW-striking quartz veins, which locally contain highly interesting Ag–Bi–Pb sulfosalt mineralisation (e.g. Paar, 2006).

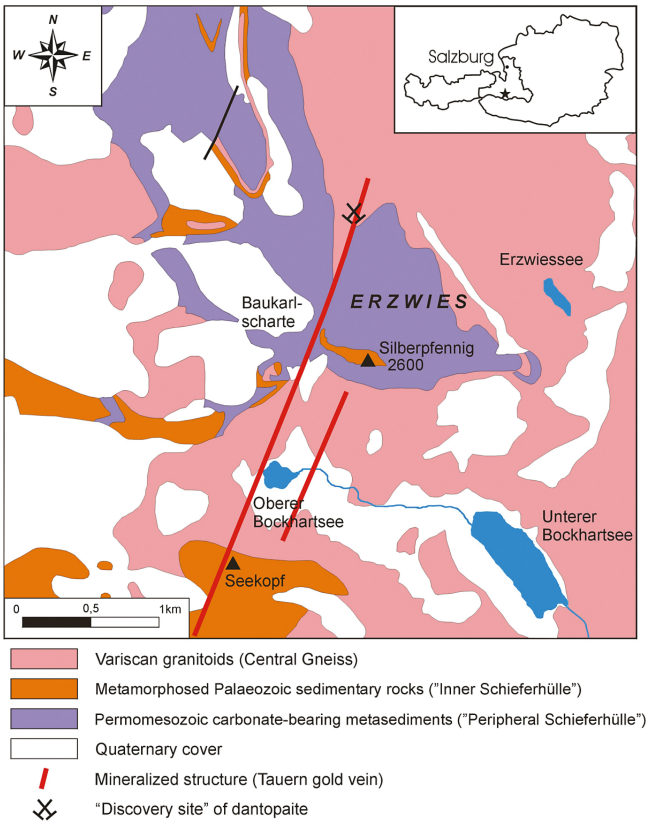

Figure 1. The geological map of the Erzwies area and the location of the erzwiesite occurrence.

The region of Erzwies ("ore meadow") was part of an important ore mining district in historical times. It is located north of the Baukarlscharte, on the western side of the Gasteiner Valley in Salzburg Province of Austria. The whole district (Siglitz–Bockhart–Erzwies) comprises an area of 5×2 km (Fig. 1). Mining for gold and silver dates back to the 14th century and even before that time (Gruber, 2006). In the 18th and 19th centuries, less important mining for lead, zinc, and iron occurred. Numerous adits, most of them collapsed, and extensive dumps are nowadays a testimony of extensive mining, which was done both from the surface and from underground.

The vein type mineralisation of the epi- to meso-thermal type was formed at the retrograde stage of the Alpine metamorphism at temperatures at and below 300 °C. A more detailed description is given in Paar (2006). Various ore types can be distinguished in the area of Erzwies. The prevail-

Figure 2. Outcrop below the Baukarlscharte with several discordant E–W trending quartz veins within Central Gneiss.

Figure 3. Photograph of a portion of the erzwiesite type specimen, deposited in the mineralogical collection of the Natural History Museum, Wien, Austria, under catalogue no. O 2407, (field of view ca. 10×8 mm), showing quartz gangue with black sulfosalt aggregates (ca. 1×3 mm in size).

ing mineralisation is (1) massive ore composed of sphalerite (coarse-grained, variously coloured); galena (with freibergite, polybasite, acanthite); and pyrite, particularly in banded sequences within a carbonate gangue (Ca–Mg–Fe–Mn carbonates). The other type (type 2) is composed of pyrite, arsenopyrite, and gold, frequently in brecciated textures together with quartz.

A third ore type (3) is represented by E–W trending sulfosalt-bearing veins of quartz which penetrate metagranitic rocks (the so-called "Central Gneiss"; Fig. 2). More than 70 veins and veinlets of this type are exposed at altitudes between 2200 and 2440 m a.s.l. and can be traced for at least several metres along strike. Their thicknesses can vary between a few centimetres and almost half a metre. A common associate is pyrite in cubes up to 10 cm and in a fine-grained, almost powdery variety. At least five of these quartz veins carry a rich sulfosalt mineralisation.

At Erzwies the sulfosalt minerals occur as needle-like single or bladed crystals and massive forms frequently intergrown as radiating aggregates. The size of the sulfosalt inclusions extend up to almost 10 cm. On the basis of a very detailed analytical study, the sulfosalt assemblage of these quartz veins (type 3) consists of bismuthinite, gladite, krupkaite, silver-rich members of the lillianite homologous series (such as vikingite, (?)treasurite, heyrovskýite, eskimoite, and ourayite), pavonite-type phases, cosalite, neyite, tetradymite, gold, and galena-matildite.

One of these veins contained dantopaite, a member of the pavonite homologous series (Makovicky et al., 2010; small exploration trench at 2275 m a.s.l.). Another quartz vein exposed at approx. 2390 m a.s.l. carries abundant sulfosalts, including the new mineral erzwiesite. A detailed treatment of the sulfosalt mineralogy at Erzwies is being prepared and will be published elsewhere.

3 Appearance and physical properties

Erzwiesite occurs together with other sulfosalts and sulfides within a single quartz vein of ore type 3 and was found only in a few specimens. This quartz vein is exposed at elevations between 2390 and 2395 m above sea level to the west of what had probably been the largest mine of this area, called "Blei Beul" or "Beim Bleibau". The outcrop of the vein is on a steep slope, where it was explored for a few metres along strike and depth. The width of the vein varies between a few centimetres up to 12 cm. The quartz is highly fractured and limonite-stained. The ore mineralisation occurs irregularly distributed within the quartz, where it forms nests of intergrown sulfosalts up to a maximum size of 5 cm (Fig. 3). In hand specimens, the dominant minerals are bismuthinite and members of the lillianite and pavonite homologous series. Their distinction by the naked eye is based on the good cleavage of bismuthinite and the poor cleavage of the associated sulfosalts. Powdery pyrite is the dominating associate.

The accompanying sulfosalts are all Bi rich and belong to the aikinite–bismuthinite series (aikinite, krupkaite) and lillianite homologous series (gustavite, vikingite, heyrovskýite, eskimoite, ourayite). Minor associates are gold (electrum), tetradymite, and galena-matildite solid solution.

Erzwiesite occurs as black anhedral crystals, with a black streak. It is non-fluorescent, opaque in transmitted light, and presents a metallic luster. It is brittle, no cleavage is observed, and the fractures are irregular. The calculated densities for empirical formulae ($Z = 1$) and unit cell parameters (from SCXRD studies) and for the crystal-structure refinement formula are 7.045 and 7.074 g cm^{-3}, respectively. Mohs' hardness is 3–3.5 (VHN_{50} ranges from 195 to 224, mean 210 kg mm^{-2}). Erzwiesite has a greyish colour in reflected light. Pleochroism is distinct white to dark grey, and

Table 1. Reflectance values (WTiC standard in air) for erzwiesite. The values recommended by the Commission of Ore Mineralogy of IMA are marked in bold.

λ (nm)	R_{min}	R_{max}	λ (nm)	R_{min}	R_{max}
400	41.9	50.1	560	41.7	44.8
420	44.7	48.1	580	41.6	44.9
440	44.6	48.4	**589**	**41.5**	**44.5**
460	44.6	48.0	600	41.1	43.9
470	**44.5**	**47.6**	620	40.5	44.1
480	44.3	47.1	640	40.5	43.6
500	43.6	46.8	**650**	**40.4**	**43.6**
520	42.4	45.7	660	40.3	43.6
540	41.8	45.1	680	40.0	43.1
546	**41.9**	**45.0**	700	40.0	43.1

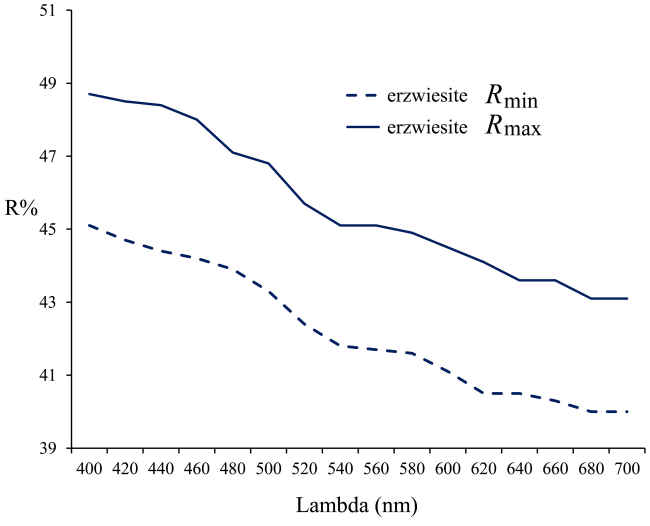

Figure 4. Reflectance data of erzwiesite.

bireflectance is weak to distinct (in oil). Anisotropy is distinct in air and becomes enhanced in oil. Between crossed polars, rotation tints change from pale brown to pale bluish grey to dark brown and are thus very similar to that of other members of the LHS. Twinning is not observed.

Reflectance value measurements taken at extinction positions in air (WTiC standard, area measured 20×20 µm), acquired with a Leitz MPV-SP microscope photometer, are given in Table 1 and are plotted in Fig. 4.

4 Chemical compositions

Chemical analyses of erzwiesite and of the associated minerals were performed at the Central Research Laboratories of the Natural History Museum, Vienna, on a JEOL "Hyperprobe" JXA 8530F field-emission gun electron microprobe (FE-EPMA). Analytical conditions were WDS measuring mode, accelerating voltage of 25 kV and 20 nA, beam current, 1.5 µm beam diameter, and count time of 15 s on peak and 5 s on background positions. JEOL and a probe for EPMA software were used for acquisition and processing of data. The following emission lines and standards were used: Ag$L\alpha$ (Ag metal), Pb$L\alpha$ (galena), Bi$L\alpha$ and S$K\alpha$ (Bi_2S_3), Sb$L\alpha$ (stibnite), Cd$L\alpha$ and Te$L\alpha$ (CdTe), Cu$K\alpha$ (chalcopyrite), and Se$L\alpha$ (Bi_2Se_3). No other elements with $Z>8$ were detected. Under the analytical conditions described, the detection limits for the measured elements in the erzwiesite matrix were as follows (expressed in wt %): S and Cu ~ 0.03; Ag, Cd, Sb, Te, and Se ~ 0.06; and Pb and Bi ~ 0.09.

Analytical data, as average chemical compositions for a specific number of measured points (NA) of four different erzwiesite grains from different areas (grain 1 to grain 4) of several polished sections, as shown in Fig. 5a, are presented in Table 2, together with the empirical formulae based on 76 apfu (36Me + 40S) and with the chemistry resulting from structural formula (SREFF) obtained from the SCXRD study. The ideal formula (IF) with resulting chemistry and calculated parameters, N_{chem}, Subst.(%), and x (Makovicky and Karup-Møller, 1977a), for all groups are also shown.

The amounts of Cu, Cd, Sb, Te, and Se are small but above detection limits. The empirical formula for the grain used for the SCXRD study is $Ag_{8.18}Cu_{0.05}Pb_{11.31}Cd_{0.12}Bi_{16.30}Sb_{0.01}S_{39.81}Te_{0.13}Se_{0.06}$, calculated based on 76 apfu. The assumption that Cu^+, Cd^{2+}, Sb^{3+}, Te^{2-}, and Se^{2-} can replace Ag^+, Pb^{2+}, Bi^{3+}, and S^{2-}, respectively, allows us to write the simplified formula as $(Ag,Cu)_{8.23}(Pb,Cd)_{11.43}(Bi,Sb)_{16.31}(S,Te,Se)_{40.03}$. The ideal formula, taking into account the simplified formula and the results of the SCXRD, is $Ag_8Pb_{12}Bi_{16}S_{40}$, which requires (in wt %) Ag 10.82, Pb 31.76, Bi 41.92, and S 16.08, totalling 100 00. Erzwiesite from Erzwies is represented by a range of compositions with a substitution percentage of $^{8.01}L_{55.6}$ to $^{7.91}L_{69}$.

Other minerals associated with erzwiesite in the polished section of Fig. 5 are treasurite $^{6.01(15)}L_{61.15(50)}$, with empirical formula $Ag_{4.51}Cu_{0.4}Pb_{10.55}Cd_{0.11}Bi_{12.88}Sb_{0.06}S_{31.88}$; heyrovskýite $^{6.88(10)}L_{59.35(4)}$, with empirical formula $Ag_{5.551}Cu_{0.35}Pb_{12.09}Cd_{0.07}Bi_{13.99}Sb_{0.07}S_{35.88}$; and galena, with empirical formula $Ag_{0.08}Pb_{0.85}Bi_{0.09}S_{0.99}$, carrying notable amounts of 3.5 Ag and 7.7 Bi (in wt %).

5 X-ray crystallography

X-ray intensity data of a small ($0.035 \times 0.045 \times 0.09$ mm) needle-shaped crystal of erzwiesite were collected at room temperature using a Bruker AXS three-circle diffractometer equipped with a CCD area detector. The SMART (Bruker AXS, 1998a) system of programs was used for unit cell determination and data collection, SAINT+ (Bruker AXS, 1998b) for the reduction of the intensity data, and XPREP (Bruker AXS, 1997) for space group determination and empirical absorption correction based on pseudo-ψ scans. The space group is *Cmcm*, as proposed by the XPREP program, and

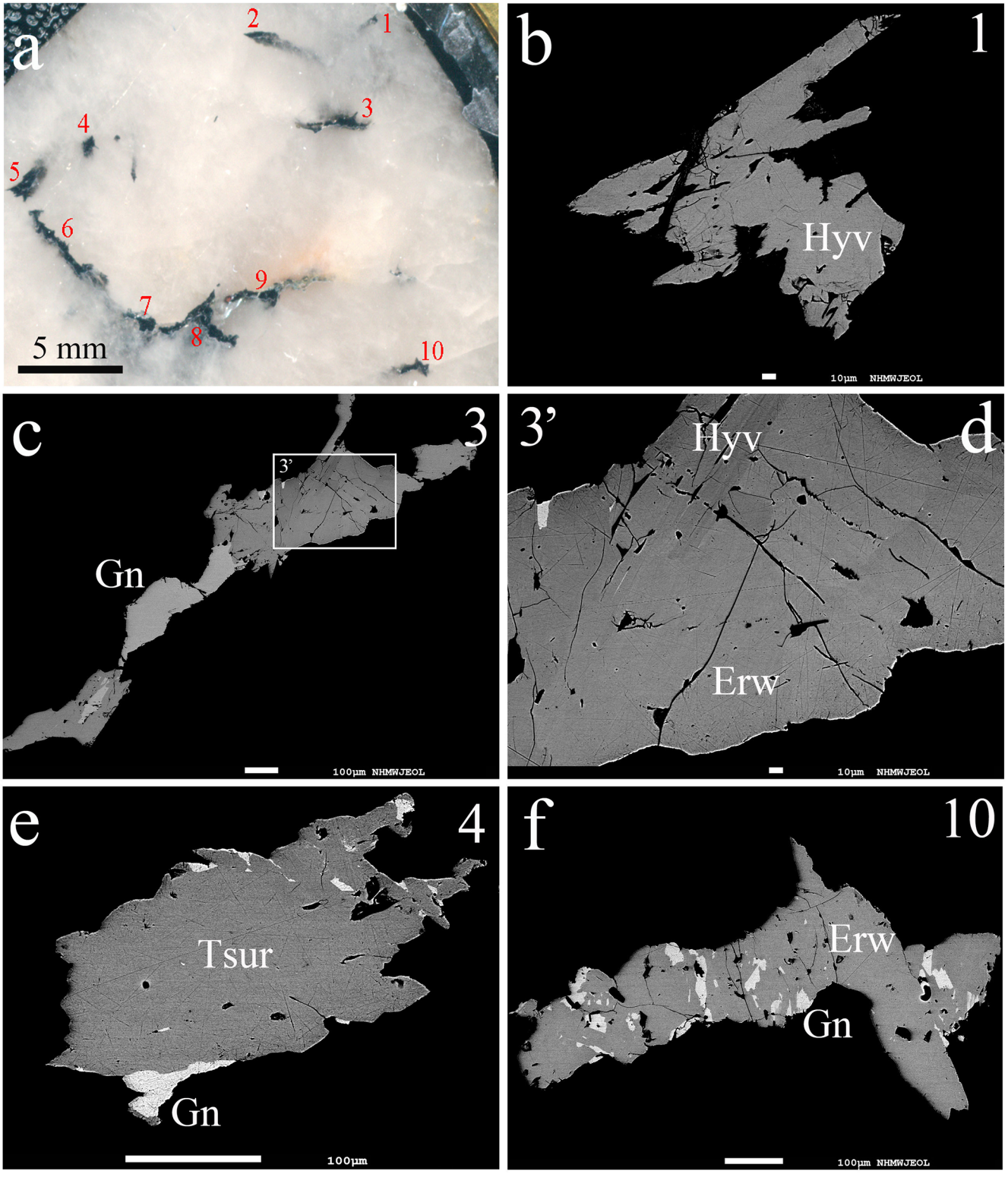

Figure 5. **(a)** Low-magnification optical image of a polished section showing 10 sulfosalt aggregates in quartz. **(b–f)** High-magnification backscattered-electron image of **(b)** aggregate 1 – homogeneous heyrovskýite (Hyv), **(c, d)** aggregate 3 – galena (Gn) and heyrovskýite (Hyv) lamellae in homogeneous erzwiesite (Erw), **(e)** galena (Gn) and treasurite (Tsur), and **(f)** galena (Gn) and erzwiesite (Erw).

Table 2. Average chemical composition data (in wt %) for erzwiesite (Erw) from Erzwies, erwiesite from Kutná Hora (KH, sample ST 22B from Pažout, 2017), and synthetic analogue (SA, Topa et al., 2010). Empirical formulae are calculated based on 76 apfu for $Z = 1$.

	Grain 1	Grain 2	Grain 3	Grain 4[a]	SREFF[b]	IF[c]	KH	SA
NA[d]	4	9	7	6	–	–	4	15
Ag	8.65(18)	9.26(13)	10.01(12)	11.10(27)	11.78	10.82	11.39	11.88
Cu	0.14(5)	0.20(5)	0.13(9)	0.04(3)	–	–	0.04	–
Pb	37.50(48)	35.23(45)	32.87(34)	29.50(77)	28.91	31.76	29.85	26.06
Cd	0.00(0)	0.14(5)	0.10(7)	0.17(1)	–	–	0.07	–
Bi	37.64(35)	39.65(24)	41.08(32)	42.90(63)	43.10	41.92	38.55	45.78
Sb	0.12(1)	0.04(2)	0.04(3)	0.00(0)	–	–	2.76	–
Te	0.20(6)	0.22(5)	0.10(12)	0.21(14)	–	–	–	–
Se	0.00(0)	0.06(3)	0.03(4)	0.08(5)	–	–	0.00	–
S	15.48(8)	15.75(9)	16.00(14)	16.08(11)	16.21	16.08	17.30	16.42
Total	99.74(46)	100.57(32)	100.38(22)	100.10(63)	100	100	99.96	100.15
Parameters calculated with at. % values								
ch[e]	0.39(8)	0.28(10)	0.08(19)	−0.01(38)	−0.42	0	−6.2	−0.53
N_{chem}[f]	8.01(15)	7.92(11)	7.84(17)	7.91(26)	8.38	8	8.08	7.34
Subst.(%)[g]	55.59(68)	59.60(59)	63.58(43	69.01(11)	70.59	66.67	69.26	75.54
x[h]	6.68(12)	7.08(12)	7.44(16)	8.16(40)	9.0	8	8.42	8.07
Formulae calculated on 76 apfu (36Me + 40S)								
Ag + Cu	6.74(7)	7.17(6)	7.57(5)	8.23(16)	8.64	8	8.16	8.66
Pb + Cd	14.81(17)	13.78(15)	12.74(14)	11.43(31)	11.04	12	11.75	9.89
Bi + Sb	14.82(15)	15.30(12)	15.72(14)	16.31(24)	16.32	16	16.17	17.22
S + Te + Se	39.63(4)	39.75(9)	39.95(17)	40.03(30)	40	40	40.39	40.24

[a] The grain used for single-crystal X-ray diffraction study. [b] Formula derived from the crystal-structure refinement. [c] Ideal formula. [d] Number of point analyses. [e] ch charge balance values calculated as (∑ cation valence − ∑ anion valence) using atomic values. [f] $N_{chem} = (2 \times A - 3)/(1–2 \times A)$, where $A = 0.5 \times (\sum Me^{2+}/100) + \sum Me^{3+}/100$ from Makovicky and Karup-Møller (1977a). [g] molar fraction of the Ag–Bi end member = Subst. % = $(1 - (2Me^{3+}/100 - A/100 - 1)/(6 \times A - 5)) \times 100$ from Makovicky and Karup-Møller (1977a). [h] substitution parameter $x = (N_{chem} - 2) \times$ Subst. %/50 in general formula $Ag_xPb_{4N-1-2x}Bi_{8+x}S_{4N+8}$ for $N = 8$ and $Z = 1$, from Makovicky and Karup-Møller (1977a).

is in accordance with the space group of all orthorhombic homologues of lillianite. The initial model was based on the coordinates and atom names of erzwiesite synthetic analogue $^8L_{70}$ (Topa et al., 2010), which contains five cation and six anion sites. The Pb2 and Bi1 sites are pure Pb and Bi sites, respectively, as in synthetic analogue $^8L_{70}$. The Pb1, Bi2, and Bi3 sites are mixed with Ag in a similar way as in synthetic analogue $^8L_{70}$ and were refined using the scattering curves of Pb and Bi against Ag.

The refinement of the structure against F^2 using SHELXL (Bruker AXS, 1997) gave the $Ag_{8.64}Pb_{9.04}Bi_{18.32}S_{40}$ ($Z = 1$) formula with overestimated Bi and underestimated Pb general content and unbalanced charge values of 2.21 and 1.68 when atomic percent and formula coefficients were used, respectively. The Bi2 site is a mixed site with $Bi_{0.70(4)}Ag_{0.30(4)}$ occupancy. Similar results were obtained for the (Bi,Ag)2 site of the synthetic analogue ($Bi_{0.742(7)}Ag_{0.258(7)}$) of erzwiesite (Topa et al., 2010), in which a certain Pb amount was suspected. Therefore, we assumed $Bi_{0.45(4)}Pb_{0.25}Ag_{0.30(4)}$ occupancy for the erzwiesite Bi2 site [$Bi_{0.70(4)}Ag_{0.30(4)}$], in accordance with the inability to distinguish between Pb and Bi (very close atomic numbers) in the diffraction study, bond length, charge distribution, and bond-valance sum values. With that adjustment, the erzwiesite formula derived from the crystal-structure refinement (SREF) becomes $Ag_{8.64}Pb_{11.04}Bi_{16.32}S_{40}$, $Z = 1$, with a better charge balance value of −0.42 and close to the EPMA empirical formula (Table 2). The displacement parameters of cation positions were refined anisotropically, while the displacement parameters of anion positions were refined isotropically due to some negatively refined ones. The structure was refined to $R_1 = 5.24\,\%$ for 308 data with $F_o > 4\sigma(F_o)$ and 51 variable parameters. Experimental and refinement conditions are specified in Table 3. The relatively low resolution of the dataset ($2\theta_{max} = 41.68°$) reflects the improper strategy of data collection for the available crystal from Madoc. Despite this limitation, the refinement converged to a stable and chemically consistent structural model, supported by agreement with chemical data and bond-valence analysis. Fractional coordinates, site occupancies, anisotropic displacement parameters, charge distribution, and bond-valence sum values are

Table 3. Crystal data and summary of parameters describing data collection and refinement for erzwiesite.

Crystal data	
Crystal size (mm)	$0.035 \times 0.045 \times 0.09$
Space group, Z	*Cmcm* (no. 63), 4
a (Å)	4.085(5)
b (Å)	13.462(15)
c (Å)	33.92(4)
V (Å^3)	1866(4)
Data collection and refinement	
Radiation, wavelength (Å)	Mo$K\alpha$, $\lambda = 0.71073$
Temperature (K)	293(2)
$2\theta_{max}$ (°)	41.68
Measured reflections	1423
Unique reflections	352
Reflections with $F_o > 4\sigma(F_o)$	308
R_{int}	0.1064
R_σ	0.0762
Range of h, k, l	$-4 \le h \le 4$, $-10 \le k \le 13$, $-31 \le l \le 34$
R_1 [$F_o > 4\sigma(F_o)$]	0.0524
R (all data)	0.0632
wR (on F_o^2)	0.1232
Goof	1.138
Number of refined parameters	51
Extinction coefficient	0.0012(2)
Maximum and minimum residual peak (e Å^{-3})	1.73 (0.81 Å from S6) / −1.66 (0.58 Å from S5)

Despite the limited data resolution ($2\theta_{max} = 41.68°$) and completeness, due to an inappropriate data collection strategy, the refinement converged to a chemically and structurally consistent model.

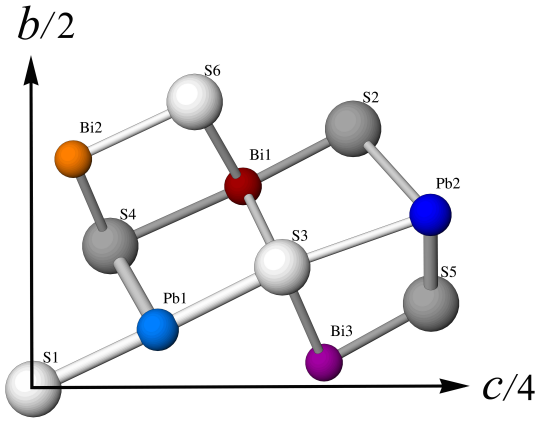

Figure 6. Atom labelling in the asymmetric unit of erzwiesite. White: S sites, dark blue: full Pb2 site, light blue: Pb1 site with site occupancy $Pb_{0.63(4)}Ag_{0.37(4)}$, red: full Bi1 site, orange: Bi2 site with site occupancy $Bi_{0.45(4)}Pb_{0.25}Ag_{0.30(4)}$, mauve: Bi3 site occupancy $Bi_{0.59(4)}Ag_{0.41(4)}$. Dark and light colours of each site represent two different a positions.

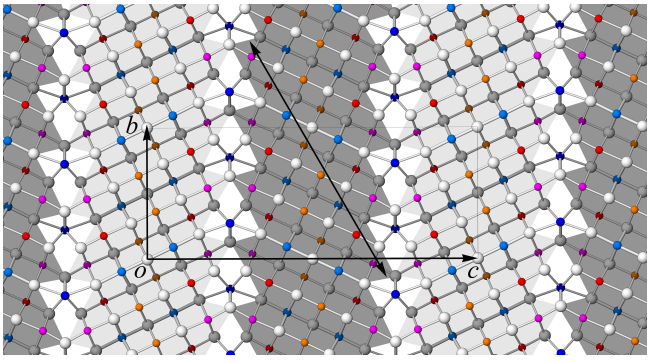

Figure 7. The crystal structure of erzwiesite viewed along [100]. Atom colouring is as in Fig. 2. The doubled arrow line indicates the eight cation polyhedra running diagonally through an individual slab.

compiled in Table 4. Table 5 reports selected cation–anion bond distances. Full details are given in the erzwiesite.CIF, erzwiesite_checkCIF.pdf, and structure factor files, all deposited as a Supplement (Supplement files S1, S2, and S3).

Powder X-ray data were not collected due to erzwiesite admixture with other members of the lillianite homologous series and galena but were calculated on the basis of the single-crystal-structure results. Data are listed in Table 6.

6 Description of the structure

The asymmetric unit of the erzwiesite structure contains five independent coordination polyhedra of cations and six of anions (Fig. 6). It contains the Pb2 site with bicapped trigonal prismatic coordination (CN = 8) in a special position and placed on the reflection planes of the space group. The other four octahedral coordination polyhedra (the Pb1 site and the Bi2 site in the centre and Bi1 site and Bi3 site at the end) form PbS-like $(311)_{PbS}$ slabs with the same width (Fig. 7). The centre of the slabs contains Pb and more Ag and less Bi (0.88 Pb, 0.67 Ag, and 0.45 Bi) than the Bi-dominant exterior of the slab (1.59 Bi and 0.41 Ag). Adjacent slabs are in a mirror-related orientation. The width of the slab is expressed by the eight metal sites in the chains of octahedra, which run diagonally across individual galena-like slabs and parallel to $[011]_{PbS}$ (Fig. 7) and defines erzwiesite as the homologue number $N = 8$ (Table 7) of the lillianite homologous series (Makovicky and Karup-Møller, 1977a, b; Moëlo et al., 2008).

The crystal data of erzwiesite (Table 7) showed same space group and similar unit cell parameters compared with the synthetic analogue $^8L_{70}$. The site occupancies for the Pb1, Bi2, and Bi3 sites in erzwiesite (Table 4) compared with the Pb1, Bi2, and Bi3 sites in the synthetic (Topa et al., 2010) phase ($(Pb_{0.53}Ag_{0.47})1$, $(Bi_{0.74}Ag_{0.26})2$, and $(Bi_{0.56}Ag_{0.44})3$) (Topa et al., 2010) indicate more Pb and less Bi and Ag.

Table 4. Sites, site occupancies (s.o.), fractional atom coordinates, anisotropic/isotropic displacement parameters (in Å^2), charge distribution, and bond valence sum values of erzwiesite.

Site	s.o.	x/a	y/b	z/c	Uaniso	TH	CD	BVS	CN
Pb1	$Pb_{0.63(4)}Ag_{0.37(4)}$	0	0.09261(18)	0.42175(7)	0.035(2)	1.63	1.651	1.672	6
Pb2	$Pb_{1.00}$	0	0.2725(2)	0.25	0.0346(13)	2.00	1.976	1.968	8
Bi1	$Bi_{1.00}$	0	0.18113(13)	0.63220(5)	0.0213(12)	3.00	2.995	2.915	6
Bi2	$Bi_{0.45(4)}Pb_{0.25}Ag_{0.30(4)}$	0	0.36318(15)	0.47434(6)	0.0272(19)	2.15	2.228	2.107	6
Bi3	$Bi_{0.59(4)}Ag_{0.41(4)}$	0	0.46007(17)	0.68273(7)	0.028(2)	2.18	2.153	2.168	6
S1	$S_{1.00}$	0	0	0.5	0.052(6)				
S2	$S_{1.00}$	0	0.0905(8)	0.7015(3)	0.021(3)				
S3	$S_{1.00}$	0	0.1910(9)	0.3431(3)	0.026(3)				
S4	$S_{1.00}$	0	0.2755(9)	0.5488(4)	0.031(3)				
S5	$S_{1.00}$	0	0.3669(16)	0.75	0.043(5)				
S6	$S_{1.00}$	0	0.4540(8)	0.3977(3)	0.023(3)				

* TH is the charge of the site obtained from refinement, and CD and BVS represent charge distribution and bond-valence sums, respectively, calculated for the cation sites with the program ECoN21 (Ilinca, 2022).

Table 5. Selected bond lengths (Å) for erzwiesite.

Pb1-		Pb2-			
S6	2.885(8) × 2	S5	2.774(15) × 2		
S4	2.885(9) × 2	S2	3.207(9) × 4		
S1	2.932(4)	S3	3.344(12) × 2		
S3	2.977(12)				
Bi1-		**Bi2-**		**Bi3-**	
S2	2.648(11)	S4	2.787(13)	S5	2.604(11)
S3	2.799(8) × 2	S6	2.873(11)	S2	2.768(8) × 2
S6	2.917(8) × 2	S4	2.877(9) × 2	S6	2.962(11)
S4	3.102(13)	S1	2.885(3) × 2	S3	3.013(9) × 2

7 Discussion

A comparison of ideal formulae, N_{chem}, the molar fraction of the Ag–Bi end member (Subst. %), and cell parameters for erzwiesite and $N = 7.5$ and $N = 7$ members of the lillianite homologous series is shown in Table 7. Aschamalmite (Callegari and Boiocchi, 2009) is an Ag-free (or Ag-low) $^{7}L_0$ monoclinic $N = 7$ member of the series, heyrovskýite is an orthorhombic $N = 7$ member of the series with chemistries varying from Ag-free $^{7}L_0$ (Pinto et al., 2011) to Ag-bearing $^{7}L_{52.8}$ (Makovicky et al., 1991), and eskimoite is an Ag-rich $^{7}L_{70}$ (Makovicky and Karup-Møller, 1977b) monoclinic $N = 7$ member of the series. Tarutinoite, recently described by Kasatkin et al. (2025), is monoclinic with a novel configuration of two different slab lengths of $N = 7$ and $N = 8$, with 7 (i.e. $N_1 \neq N_2$ and $N = (N_1 + N_2)/2 = 7.5$) and chemistry characterised by $^{7.5}L_{54.6}$, similar to the configuration $N_1 \neq N_2$ and $N = (4+7)/2 = 5.5$ found in vikingite $^{5.5}L_{71.4}$. Although the ideal formulae (and also structure-derived formulae) for chemistry of erzwiesite ($^{8}L_{66.6}$) and its synthetic analogue ($^{8}L_{75}$) are relatively close to one another, their experimentally measured ranges are different. The synthetic analogue is homogenous (SH Table 2) with very limited variations (Topa et al., 2010), in contrast with the erzwiesite chemistry, which ranges from $^{8.01}L_{55.6}$ to $^{7.91}L_{69}$.

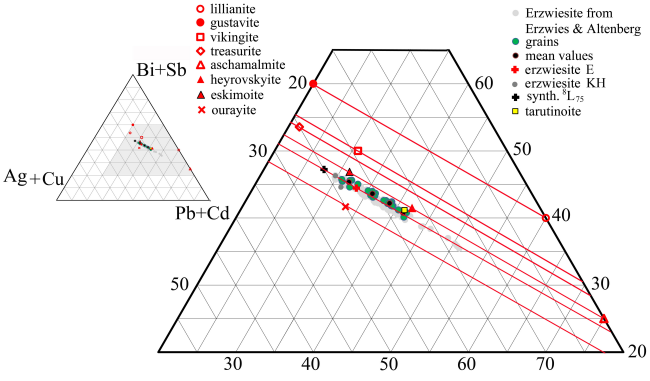

Figure 8. Ternary plot in the system (Bi + Sb)–(Ag + Cu)–(Pb + Cd) depicting the position of erwiesite from Erzwies (E), erwiesite from Kutná Hora (KH), and the synthetic $^{8}L_{70}$ phase, all with $N = 8$ and tarutinoite with $N = 7.5$, amongst the known members of the lillianite homologous series with $N = 4$ (lillianite and gustavite), $N = 5.5$ (vikingite), $N = 6$ (treasurite), $N = 7$ (aschamalmite, heyrovskýite, eskimoite), and $N = 11$ (ourayite).

Besides the Erzwies mining area, erzwiesite was described from the Kutná Hora ore district, Czech Republic, by Pažout (2017), where it contains 1.95 to 2.96 Sb wt % and has a limited chemical variation expressed by $^{8.68}L_{68.8}$ to $^{8.06}L_{71.8}$. The degree of its substitution lies between those of synthetic analogue in the upper side and erzwiesite in the lower side of the range. Moreover, a long time after the publication of the sulfosalt chemistry from the Altenberg mining district, Salzburg Province, Austria, by Putz et al. (2003), we realised that regarding the group of chemistries showing $N = 7$ to $N = 12$ members of the lillianite homogenous series, there

Table 6. Calculated X-ray powder diffraction data (d in Å) for erzwiesite.

$I_{rel.}$	d_{calc}/Å	h	k	l	$I_{rel.}$	d_{calc}/Å	h	k	l	$I_{rel.}$	d_{calc}/Å	h	k	l
5	16.96	0	0	2	4	2.421	1	1	11	12	1.7378	1	7	1
3	8.48	0	0	4	3	2.173	1	5	4	8	1.7371	2	4	2
5	4.33	0	2	6	36	2.170	1	1	13	7	1.7353	1	3	16
5	3.809	1	1	2	3	2.120	0	0	16	22	1.7352	2	2	9
64	**3.588**	**0**	**2**	**8**	16	2.089	1	5	6	5	1.7310	1	7	2
33	3.550	1	1	4	11	2.085	0	6	6	2	1.7198	1	7	3
98	**3.387**	**1**	**1**	**5**	38	2.059	1	1	14	12	1.7163	0	4	17
3	3.366	0	4	0	39	2.043	2	0	0	5	1.7031	1	5	13
37	**3.349**	**0**	**4**	**1**	**43**	**2.039**	**1**	**5**	**7**	2	1.7012	0	6	13
30	3.301	0	4	2	23	2.036	0	6	7	2	1.6960	0	0	20
85	**3.288**	**0**	**2**	**9**	17	1.9862	1	5	8	9	1.6936	2	2	10
7	3.226	0	4	3	6	1.9832	0	6	8	8	1.6645	0	8	3
34	3.215	1	1	6	2	1.9663	0	4	14	10	1.6509	2	2	11
36	3.029	0	2	10	5	1.9574	1	1	15	7	1.6506	0	8	4
8	3.021	1	3	0	3	1.8900	1	3	14	2	1.6442	0	4	18
5	3.009	1	3	1	10	1.8844	0	0	18	3	1.5145	0	4	20
24	2.974	1	3	2	5	1.8166	1	5	11	3	1.4928	1	1	21
100	**2.919**	**1**	**3**	**3**	3	1.8143	0	6	11	5	1.4593	2	6	6
2	2.874	1	1	8	14	1.8103	1	3	15	5	1.4562	0	4	21
99	**2.846**	**1**	**3**	**4**	4	1.7938	0	4	16	12	1.4421	2	6	7
34	2.803	0	2	11	15	1.7751	2	2	8	3	1.4229	2	6	8
7	2.760	1	3	5	10	1.7595	1	5	12	6	1.3851	2	0	18
4	2.664	1	3	6	5	1.7574	0	6	12	4	1.3798	1	1	23
4	2.606	0	2	12	10	1.7439	2	4	1	6	1.3733	1	3	22

The theoretical pattern was calculated using PowderCell 2.3 (Kraus and Nolze, 1996) in the Debye–Scherrer configuration employing Cu$K\alpha$ radiation ($\lambda = 1.540598$ Å), a fixed slit, and no anomalous dispersion. Unit-cell parameters, space group, atom positions, site-occupancy factors, and equivalent displacement factors from the crystal-structure determination were used. The seven strongest lines are indicated in bold.

Table 7. Comparative data for erzwiesite ($N = 8$) and for $N = 7.5$ and $N = 7$ members of the lillianite homologous series ($Z = 1$).

Mineral ^{N1,N2}L[a]	Erzwiesite, ^{8,8}L	Synthetic ^{8,8}L	Tarutinoite ^{7,8}L	Eskimoite[b] ^{5,9}L	Heyrovskýite ^{7,7}L	Aschamalmite[b] ^{7,7}L
Ideal formula	$Ag_8Pb_{12}Bi_{16}S_{40}$	$Ag_9Pb_{10}Bi_{17}S_{40}$	$Ag_6Pb_{14}Bi_{14}S_{38}$	$Ag_7Pb_{10}Bi_{15}S_{36}$	$Ag_{5.28}Pb_{13.44}Bi_{13.28}S_{36}$	$Pb_{24}Bi_8S_{36}$
N	8	8	7.5	7	7	7
Substitution (%)	66.67	75	54.55	70	52.8	0
Crystal system	orthorhombic	orthorhombic	monoclinic	monoclinic	orthorhombic	monoclinic
Space group	*Cmcm*	*Cmcm*	*C*2/*m*	*C*2/*m*	*Cmcm*	*C*2/*m*
Cell parameters						
a	4.085(5)	4.084(1)	4.10y(1)	4.1	4.110(1)	4.13
b	13.46(2)	13.453(4)	13.55x(4)	13.46	13.600(3)	13.72
c	33.92(4)	33.932(9)	54.6xx(9)	30.49	30.485(12)	31.42
α, β, γ	90, 90, 90	90, 90, 90	90, 96.4, 90	90, 93.4, 90	90, 90, 90	90, 90.9, 90
R_1 factor (%)	5.24	3.66	13.66	–	6.2	
Ref.[c]	1	2	3	4	5	6

[a] ^{N1,N2}L are homologues of the lillianite series, where N_1 and N_2 are the number of metal sites in two alternating slabs, and $N = (N_1 + N_2)/2$ is the homologue number. [b] Crystal structure unknown, structure model only. [c] References: (1) this study, (2) Topa et al. (2010), (3) Kasatkin et al. (2025), (4) Makovicky and Karup-Møller (1977b), (5) Makovicky et al. (1991), and (6) Callegari and Boiocchi (2009).

was a group characterised by $^{8.09–8.15}L_{40.1–72.3}$, representing the first measurements of erzwiesite. Ag-free and Ag-high (more than synthetical analogue) erzwiesite chemistries were not found until now. The grains possessing low substitution values were difficult to extract for the single-crystal study, and, therefore we cannot predict the system of crystallisation and space groups of Ag-free and Ag-high erzwiesite chemistries.

A ternary plot of the system, (Bi + Sb) – (Ag + Cu) – (Pb + Cd), depicting the position of erwiesite ($N = 8$) and

the other known members of the lillianite homologous series is given in Fig. 8. The chemistry of erzwiesite from Altenberg (grey background) exceeds both sides of the chemistry of type erzwiesite from Erzwies but remains under the chemistry of synthetic analogue of erzwiesite.

The plotting process in the ternary diagram of the chemistries obtained by the EMPA method, as well as the values of N_{chem} provided by them, will together give a first indication of the identification of the homologue number for a mineral belonging to the lillianite homologous series. The quality of Pb and Bi(Sb) element determination is crucial because the calculation of N_{chem} is based on them. The results of the single-crystal study will provide the real answer about the homologue number and will give the correct identification of the phase. For example, the calculated N_{chem} for the synthetic $^{8}L_{70}$ phase is 7.34 (Table 2), in contrast with the result of the single-crystal study, which clearly shows $N = 8$.

Data availability. Crystallographic data for erzwiesite are available in the Supplement.

Supplement. The supplement related to this article is available online at https://doi.org/10.5194/ejm-38-237-2026-supplement.

Author contributions. DT and WHP initiated the project. DT and HP performed EMPA, HP and GZ performed optical measurements, and DT performed the SCXRD experiment. All authors interpreted the obtained data. The paper was written by DT with contributions from all co-authors.

Competing interests. The contact author has declared that none of the authors has any competing interests.

Disclaimer. Publisher's note: Copernicus Publications remains neutral with regard to jurisdictional claims made in the text, published maps, institutional affiliations, or any other geographical representation in this paper. The authors bear the ultimate responsibility for providing appropriate place names. Views expressed in the text are those of the authors and do not necessarily reflect the views of the publisher.

Acknowledgements. The authors are thankful to Mag. Giorgio Höfer and Mag. Georg Zagler for fieldwork and for providing sulfosalt-bearing samples, to Ministerialrat Dipl.-Ing. Erwin Leitner for his help with logistics and information about the mining history at Erzwies, and to Goran Batic for help with the sample preparation. We thank the editor Cristian Biagioni for handling the manuscript and Richard Pažout and the anonymous reviewer for their critical remarks that have improved the paper.

Review statement. This paper was edited by Cristian Biagioni and reviewed by Richard Pažout and one anonymous referee.

References

Bruker AXS: SHELXTL, Version 5.1. Bruker AXS, Inc., Madison, WI 53719, USA, 1997.

Bruker AXS: SMART, Version 5.0. Bruker AXS, Inc., Madison, WI 53719, USA, 1998a.

Bruker AXS: SAINT, Version 5.0. Bruker AXS, Inc., Madison, WI 53719, USA, 1998b.

Callegari, A. M. and Boiocchi, M.: Aschamalmite ($Pb_6Bi_2S_9$): crystal structure and ordering scheme for Pb and Bi atoms), Min. Mag., 73, 83–94, https://doi.org/10.1180/minmag.2009.073.1.83, 2009.

Ilinca, G.: Charge Distribution and Bond Valence Sum Analysis of Sulfosalts – The ECoN21 Computer Program, Minerals, 12, 924, https://doi.org/10.3390/min12080924, 2022.

Ferraris, G., Makovicky, E., and Merlino, S.: Crystallography of Modular Materials, vol. 15 of IUCr, Monographs on Crystallography, Oxford, Oxford University Press, ISBN 978-0-19-954569-8, https://doi.org/10.1107/S0108768108025986, 2008.

Gruber, F.: Der Edelmetallbergbau in Salzburg und Oberkärnten bis zum Beginn des 19.Jahrhunderts, in: Das Buch vom Tauerngold, Herausgeber:innen: Paar, W. H., Günther, W., and Gruber, F., Anton Pustet Verlag, Salzburg, Austria, 193–364, ISBN-13 9-783-7025-0536-3, 2006.

Höfer, G.: Genese der Silber-Blei-Zink-Lagerstätten im Erzwies-Revier bei Bad Hofgastein, Salzburg, Unveröffentl. Endbericht, 2001, S. 43, 2001.

Höfer, G.: Der Karst auf der Erzwies. Die Höhle, 56. Jg., Heft 1–4, 3–12, 2005.

Kasatkin, A., Biagioni, B., Nestola, F., Skoda, R., Gurzhiy, V., Agakhanov, A. A., and Kuznetsov, A.: Tarutinoite, Ag3Pb7Bi7S19, a new member of the lillianite homologous series from the Tarutinskoe copper-skarn deposit, Southern Urals, Russia, Mineral. Mag., 89, 483–491, https://doi.org/10.1180/mgm.2025.1, 2025.

Kraus, W. and Nolze, G.: POWDER CELL-A Program for the Representation and Manipulation of Crystal Structure and Calculation of the Resulting X-Ray Powder Pattern, J. Appl. Crystallogr., 29, 301–303, https://doi.org/10.1107/S0021889895014920, 1996.

Makovicky, E. and Karup-Møller, S.: Chemistry and crystallography of the lillianite homologous series. Part I: General properties and definitions. Neues Jahrbuch für Mineralogie, Abhandlung, 130, 264–287, 1977a.

Makovicky, E. and Karup-Møller, S: Chemistry and crystallography of the lillianite homologous series. Part II: Definition of new minerals: eskimoite, vikingite, ourayite and treasurite. Redefinition of schirmerite and new data on the lillianite–gustavite solid-solution series, Neues Jahrbuch für Mineralogie, Abhandlung, 131, 56–82, 1977b.

Makovicky, E., Mumme, W. G., and Hoskins, B. F.: The crystal structure of Ag–Bi-bearing heyrovskýite, Can. Mineral., 29, 553–559, 1991.

Makovicky, E.: Crystal structures of sulfides and other chalcogenides, Reviews in Mineralogy and Geochemistry, 61, 7–125, https://doi.org/10.2138/rmg.2006.61.2, 2006.

Makovicky, E., Paar, W. H., Putz, H., and Zagler, G.: Dantopaite, $Ag_5Bi_{13}S_{22}$, the ^{6}P Natural Member of the Pavonite Homologous Series, from Erzwies, Austria, Can. Mineral., 48, 467–481, https://doi.org/10.3749/canmin.48.3.467, 2010.

Makovicky, E. and Topa, D.: Lillianites and andorites: new life for the oldest homologous series of sulfosalts, Mineral. Mag., 78, 387–414, https://doi.org/10.1180/minmag.2014.078.2.11, 2014.

Moëlo, Y., Makovicky, E., Mozgova, N. N., Jambor, J. L., Cook, N., Pring, A., Paar, W. H., Nickel, E. H., Graeser, S., Karup-Møller, S., Balic-Žunic, T., Mumme, W. G., Vurro, F., Topa, D., Bindi, L., Bente, K., and Shimizu, M.: Sulfosalt systematics: a review. Report of the sulfosalt sub-committee of the IMA Commission on Ore Mineralogy, Eur. J. Mineral., 20, 7–62, https://https://doi.org/10.1127/0935-1221/2008/0020-1778, 2008.

Paar, W. H.: Montangeologie des Tauerngoldes, in: Das Buch vom Tauerngold, Herausgeber:innen: Paar, W. H., Günther, W., and Gruber, F., Anton Pustet Verlag, Salzburg, Austria, 47–192, ISBN 13 9-783-7025-0536-3, 2006.

Pinto, D., Balic-Zunic, T., Garavelli, A., and Vurro, F.: Structure refinement of Ag-free heyrovskýite from Vulcano (Aeolian Islands, Italy), Am. Mineral., 96, 1120–1128, 2011.

Pažout, R.: Lillianite homologues from Kutná Hora ore district, Czech Republic: a case of large scale Sb for Bi substitution, J. Geosci., 62, 37–57, https://doi.org/10.3190/jgeosci.235, 2017.

Putz, H., Paar, W. H., Topa, D., Höfer, G., and Lüders, V.: Structurally controlled gold and sulfosalt mineralization: the Altenberg example, Salzburg Province, Austria, Mineral. Petrol., https://doi.org/10.1007/s00710-002-0230-3, 2003.

Topa, D., Makovicky, E., Schimper, H. J., and Dittrich H.: The crystal structure of a synthetic orthorhombic $N = 8$ member of the lillianite homologous series, Can. Mineral., 48, 1127–1135, https://doi.org/10.3749/canmin.48.5.1127, 2010.

Topa, D., Makovicky, E., Zagler, G., Putz, H., and Paar, W. H.: Erzwiesite, IMA 2012-082, CNMNC Newsletter No. 15, Min. Mag., 77, 11, https://doi.org/10.1180/minmag.2013.077.1.01, 2013.